

## IMMUNOBIOLOGY AND IMMUNOTHERAPY

## Flotetuzumab and other T-cell immunotherapies upregulate MHC class II expression on acute myeloid leukemia cells

Joseph C. Rimando,<sup>1</sup> Ezhilarasi Chendamarai,<sup>1</sup> Michael P. Rettig,<sup>1</sup> Reyka Jayasinghe,<sup>1</sup> Matthew J. Christopher,<sup>1</sup> Julie K. Ritchey,<sup>1</sup> Stephanie Christ,<sup>1</sup> Miriam Y. Kim,<sup>1</sup> Ezio Bonvini,<sup>2</sup> and John F. DiPersio<sup>1</sup>

<sup>1</sup>Division of Oncology, Department of Medicine, Washington University School of Medicine, St. Louis, MO; and <sup>2</sup>MacroGenics, Inc, Rockville, MD

## KEY POINTS

- T-cell immunotherapies targeting AML antigens upregulate MHC-II expression on AML cells.
- IFN- $\gamma$  mediates the T-cell immunotherapy-induced MHC-II upregulation on AML cells.

**Acute myeloid leukemia (AML) relapse is one of the most common and significant adverse events following allogeneic hematopoietic cell transplantation (HCT). Downregulation of major histocompatibility class II (MHC-II) surface expression on AML blasts may represent a mechanism of escape from the graft-versus-malignancy effect and facilitate relapse. We hypothesized that T-cell immunotherapies targeting AML antigens would upregulate MHC-II surface expression via localized release of interferon gamma (IFN- $\gamma$ ), a protein known to upregulate MHC-II expression via JAK-STAT signaling. We demonstrate that flotetuzumab (FLZ), a CD123  $\times$  CD3 bispecific DART molecule, and chimeric antigen receptor expressing T cells targeting CD123, CD33, or CD371 upregulate MHC-II surface expression in vitro on a THP-1 AML cell line with intermediate MHC-II expression and 4 primary AML samples from patients relapsing after HCT with low MHC-II expression. We additionally show that FLZ upregulates MHC-II expression in a patient-derived xenograft model and in patients with relapsed or refractory AML who were treated with FLZ in a clinical trial. Finally, we report that FLZ-induced MHC-II upregulation is mediated by IFN- $\gamma$ . In conclusion, we provide evidence that T-cell immunotherapies targeting relapsed AML can kill AML via both MHC-independent mechanisms and by an MHC-dependent mechanism through local release of IFN- $\gamma$  and subsequent upregulation of MHC-II expression.**

## Introduction

Patients with acute myeloid leukemia (AML) that relapses after allogeneic hematopoietic cell transplantation (allo-HCT) have dismal outcomes.<sup>1-4</sup> Approximately 30% to 50% of patients with AML who relapse after allo-HCT exhibit major histocompatibility class II (MHC-II) downregulation.<sup>5,6</sup> AML blasts with downregulated MHC-II expression fail to stimulate HLA-mismatched T cells in vitro, suggesting that decreased MHC-II expression may promote immune effector evasion, abrogate the graft-versus-malignancy effect, and promote disease relapse.<sup>5,6</sup>

Interferon gamma (IFN- $\gamma$ ) can restore MHC-II expression.<sup>5,7,8</sup> T-cell immunotherapies targeting AML antigens such as a flotetuzumab (FLZ), a CD123  $\times$  CD3 bispecific DART molecule, facilitate T-cell activation and localized IFN- $\gamma$  release in the presence of AML blasts in addition to MHC-independent killing.<sup>9,10</sup> We hypothesized that AML-directed T-cell immunotherapies upregulate MHC-II on AML blasts by activating T cells to locally release IFN- $\gamma$ .

## Study design

## T-cell immunotherapies and AML cells

FLZ was provided by MacroGenics (Rockville, MD). Human THP-1 cells (American Tissue Culture Collection, Manassas, VA), and primary AML samples with low MHC-II expression at diagnosis and post-HCT relapse were obtained and cultured as previously described.<sup>5,11,12</sup> Human CD3<sup>+</sup> T lymphocytes were obtained by negative immunomagnetic selection (AutoMACS; Miltenyi Biotec, Auburn, CA).<sup>5,13</sup> CD123-, CD33-, and CD371-directed chimeric antigen receptor (CAR) T cells were generated with a PLVM vector and a third-generation CD28-4-1BB-CD3 $\zeta$  CAR construct.<sup>14</sup> IFN- $\gamma$  receptor-1 (IFN- $\gamma$ R1) and  $\beta$ -actin knockout (KO) THP-1 cell lines were generated using CRISPR-Cas9 as previously described.<sup>15</sup> Serial HLA-DR expression patterns, AML blast counts, and IFN- $\gamma$  serum concentrations from patients treated with FLZ on a phase I to II study (NCT02152956) were obtained as previously described in accordance with the Declaration of Helsinki as per research protocols approved by the institutional review boards of the participating institutions. All participants provided informed consent prior to study enrollment.<sup>16-18</sup>

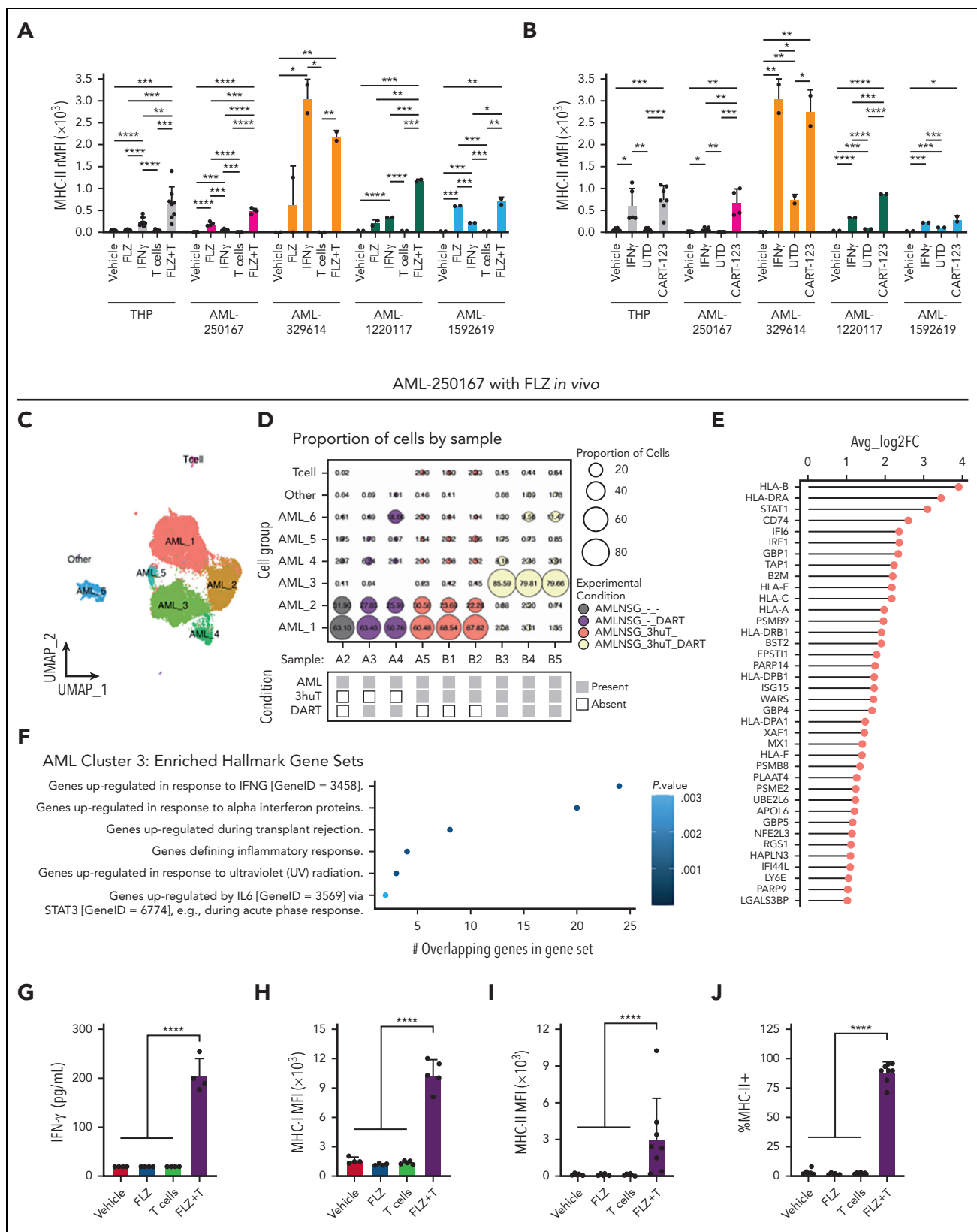


**Figure 1. AML-directed T-cell immunotherapies upregulate MHC-II expression on human AML cell lines and primary human AML cells *in vitro* and *in vivo*.** (A) Human THP-1 and primary AML cells from patient 250167, 329614, 1220117, or 1592619 were treated with vehicle (PBS), 10 ng/mL FLZ, 50 ng/mL IFN- $\gamma$ , human HLA-mismatched CD3<sup>+</sup> T cells (E:T of 1:1), or FLZ and human T cells (FLZ + T) for 48 hours. Twenty-five thousand AML cells were plated per well. MHC-II relative median fluorescence intensity (rMFI) (A) on the THP-1 and AML cells was measured via multiparametric flow cytometry. (B) THP-1, AML-250167, AML-329614, 1220117, or 1592619 cells were treated with vehicle (PBS), 50 ng/mL IFN- $\gamma$ , human UTD T cells (UTD; E:T of 0.1:1), or human T cells expressing a CAR targeting CD123 (CART-123; E:T of 0.1:1) for 48 hours. MHC-II rMFI was measured by flow cytometry. (C-J) NSG-S mice were sublethally irradiated with 250 rads and injected with 10<sup>6</sup> human AML-250167 cells per mouse. After 5.5 weeks, mice were treated with vehicle

## In vitro experiments

AML cells were cultured with 10 IU/mL interleukin-2 at the indicated effector-to-target (E:T) ratios, and IFN- $\gamma$  (PeproTech, Rocky Hill, NJ) was used as a positive control.<sup>9,10</sup> Flow cytometry measuring MHC-II and MHC-I expression was performed using BV421-labeled anti-human HLA-DR, HLA-DP, HLA-DQ (clone Tu39; BD Biosciences) and allophycocyanin-labeled anti-human HLA-A, HLA-B, HLA-C (clone W6/32, BD Biosciences), respectively.<sup>5,19</sup> Flow cytometry was also used to measure live single cell counts using SPHERO AccuCount fluorospheres (Spherotech Inc). Luminex assays (Millipore Sigma, Rockville, MD) measured IFN- $\gamma$ . Inhibition studies used anti-human IFN- $\gamma$  (clone B27; BioLegend); anti-human IFN- $\gamma$ R1 (Invitrogen #PA5-47866); companion isotype antibodies (clone MOPC-21, BioLegend and goat immunoglobulin G, Invitrogen); ruxolitinib (Selleck Chemicals, Houston, TX); and baricitinib (ApexBio Technology, Houston, TX). For T-cell activation studies, THP-1 cells were treated with IFN- $\gamma$  2 ng/mL (or vehicle) for 24 hours and then washed. THP-1 cells were subsequently replated with HLA-mismatched CD4<sup>+</sup> T cells, and T-cell proliferation was measured via carboxyfluorescein diacetate succinimidyl ester dilution using flow cytometry.

## In vivo studies

NOD-*scid* IL2R $\gamma$  null mice (Jackson Laboratory, #013062) expressing human interleukin-3, granulocyte-macrophage colony-stimulating factor, and stem cell factor (NSG-S) were irradiated with 250 rads and injected with 10<sup>6</sup> primary AML cells per mouse. After 5.5 weeks, mice were treated, killed 48 hours later, and analyzed for human AML engraftment and phenotype by flow cytometry. Single-cell RNA sequencing (scRNA-seq) was performed on human cells isolated by immunomagnetic selection.

## Single-cell RNA sequencing analyses

FASTQs were processed with Cell Ranger v6.0.1 “count” command using default parameters and GRCh38 to 2020-A reference. Data were preprocessed, scaled, normalized, and merged using Seurat v4.1.0.<sup>20</sup> Cell types were assigned based on marker expression, including T cells (*CD3D*, *CD3E*, *CD3G*) and AML cells (*KIT*, *CD33*, *IL3RA*). For cell-level and cluster-level differential expression, the “SCT” assay of “FindAllMarkers” was used. To evaluate enriched hallmark gene sets, 38 differentially expressed genes were surveyed using the molecular signatures database hallmark gene sets.

## Results and discussion

### AML-directed T-cell immunotherapies upregulate MHC-II expression on human AML cells

THP-1 express CD123 and intermediate levels of MHC-II at baseline (supplemental Figure 1). The combination of FLZ and human third-party HLA-mismatched CD3<sup>+</sup> T cells (FLZ + T) upregulated MHC-II surface expression on THP-1 cells by an average of 16-fold (Figure 1A; *P* < .005) when compared with

THP-1 cells cultured with vehicle (phosphate-buffered saline [PBS]), FLZ, or T cells alone. IFN- $\gamma$  also upregulated MHC-II by an average of sixfold (Figure 1A; *P* < .0001) when compared with vehicle controls. FLZ + T led to significant killing of THP-1 compared with controls (supplemental Figure 2). Coculture experiments were repeated with 4 CD123-expressing primary human AML samples expressing low MHC-II expression at the time of relapse after allo-HCT (AML-250167, AML-1220117, AML-1592619) or at diagnosis (AML-329614) and again demonstrated that FLZ + T upregulated MHC-II expression (244-fold for AML-250167, *P* < .00005; 548-fold for AML-329614, *P* < .005; 34-fold for AML-1220117, *P* < .001; and 34-fold for AML-1592619, *P* < .01) compared with T cells alone (Figure 1A). As these primary AML samples contain autologous T cells (E:T ratios ranging from 1:4 to 1:61), addition of FLZ alone also upregulated MHC-II (Figure 1A).

THP-1 and primary AML samples were next cocultured with human CD3<sup>+</sup> T cells transduced to express a CD123 CART (CART-123). CART-123 cells upregulated MHC-II on THP-1 (16.2-fold, *P* < .0005), AML-250167 (169-fold, *P* < .0005), AML-329614 (fourfold, *P* < .05), AML-1220117 (12-fold, *P* < .0001), and AML-1592619 (threefold, *P* < .001) cells when compared with the untransduced (UTD) T-cell controls (Figure 1B). CART-123 led to significant killing of THP-1 compared with controls (supplemental Figure 2). MHC-II upregulation was observed with CAR expressing T cells (CAR-T) cells targeting CD33 (CART-33) or CD371 (CART-371) (supplemental Figure 3).

NSG-S mice were engrafted with AML-250167 cells for 5.5 weeks and divided into 4 treatment groups: (1) vehicle, (2) FLZ, (3) human HLA-mismatched CD3<sup>+</sup> T cells, and (4) FLZ and T cells. AML-250167 cells engrafted primarily in the bone marrow (supplemental Figure 4). Plasma was collected from blood before euthanasia (48 hours posttreatment). Using scRNA-seq, 34 793 human cells purified from the bone marrow of the mice revealed 6 clusters of human AML cells and 1 human T-cell cluster (Figure 1C). Approximately 80% of AML cells from mice treated with FLZ and T cells were concentrated in cluster 3 (AML\_3), and AML cells from the control groups were concentrated in clusters AML\_1 and AML\_2 (Figure 1C-D). Upregulated genes in AML\_3 included (Figure 1E) all MHC-I antigens (*HLA-A*, *HLA-B*, *HLA-C*), nonclassical MHC-I antigens (*HLA-E*, *HLA-F*), and MHC-II antigens (*HLA-DRA*, *HLA-DRB*, *HLA-DPA1*, *HLA-DPB1*). Upregulated gene sets in AML\_3 included IFN- $\gamma$  response genes (Figure 1F). Concordant with scRNA-seq analyses, IFN- $\gamma$  plasma levels (Figure 1G) and surface expression of MHC-I and MHC-II on the human AML cells were significantly increased in mice treated with T cells and FLZ (Figure 1H-J).

Serial HLA-DR expression patterns of selected refractory AML patients treated with FLZ in a phase I to II study were also evaluated.<sup>16-18</sup> A subset of patients had a transient increase in HLA-DR expression over the course of a 28-day FLZ infusion; a subset had a sustained increase; and a subset had a sustained

**Figure 1 (continued)** (PBS), 2 mg/kg FLZ, 1 × 10<sup>7</sup> human HLA-mismatched CD3<sup>+</sup> T cells, or FLZ (1 hour after T-cell injection) and human T cells (FLZ + T) for 48 hours. (C) A Uniform Manifold Approximation and Projection for Dimension Reduction (UMAP) plot depicts scRNA-seq data from 34 793 high-quality human AML and T cells harvested from the bone marrow. (D) Proportions of cells (size of circle) for each single cell cluster were broken down by treatment group. (E) Differentially expressed genes (DEG) in AML\_3 cluster relative to all other AML clusters. (F) MSigDB hallmark gene sets enriched from AML\_3 DEGs. (G) Plasma levels of IFN- $\gamma$ . (H-J) MHC-I (H) and MHC-II (I) MFI and the percentage of MHC-II positive (J) human AML cells in the bone marrow of NSG-S mice were determined by flow cytometry. Bars represents means and error bars represent standard errors above and below (when applicable) the mean. *P* values were calculated using an unpaired, 2-sided Student *t* test. \**P* < .05; \*\**P* < .001; \*\*\**P* < .0001; \*\*\*\**P* < .00001.

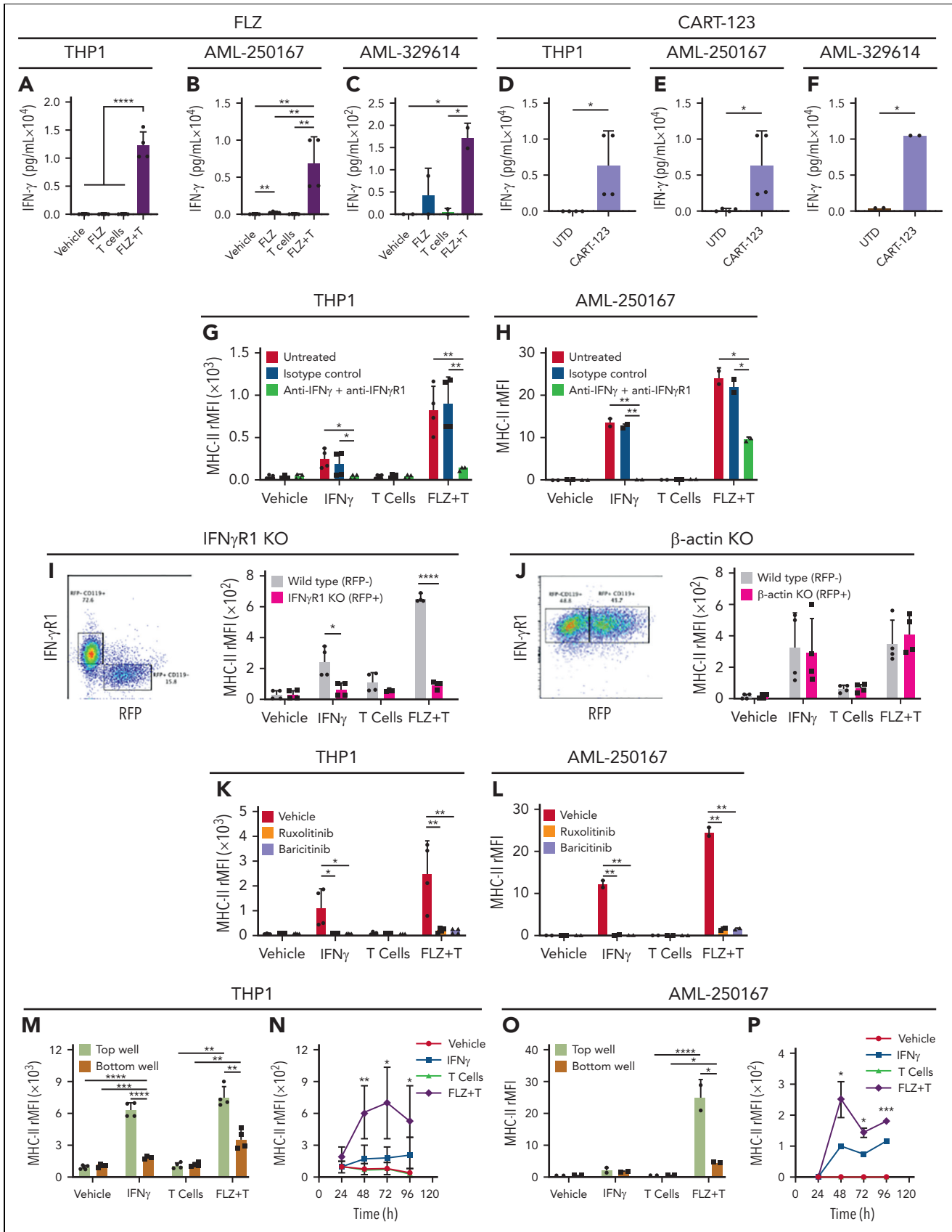


**Figure 2. T-cell immunotherapy-induced MHC-II expression is mediated by IFN- $\gamma$ .** (A-C) Human THP-1, AML-250167, or AML-329614 cells were treated with vehicle (PBS), 10 ng/mL FLZ, human HLA-mismatched CD3<sup>+</sup> T cells (E:T of 1:1), or FLZ and human T cells (FLZ + T) for 48 hours. Supernatant IFN- $\gamma$  concentrations were measured by enzyme-linked immunosorbent assay (ELISA). (D-F) THP-1, AML-250167, or AML-329614 cells were treated with human UTD T cells (E:T of 0.1:1), or human T cells expressing CART-123 (E:T of 0.1:1) for 48 hours. Supernatant IFN- $\gamma$  concentrations were measured by ELISA. (G-H) THP-1 (G) or AML-250167 (H) cells were treated with vehicle (PBS), 50 ng/mL IFN- $\gamma$ , 50 ng/mL IFN- $\gamma$  + anti-IFN- $\gamma$ R1, or 50 ng/mL IFN- $\gamma$  + anti-IFN- $\gamma$ R1 + T cells for 48 hours. (I) THP-1 cells were treated with vehicle (PBS), 50 ng/mL IFN- $\gamma$ , 50 ng/mL IFN- $\gamma$  + anti-IFN- $\gamma$ R1, or 50 ng/mL IFN- $\gamma$  + anti-IFN- $\gamma$ R1 + T cells for 48 hours. (J) AML-250167 cells were treated with vehicle (PBS), 50 ng/mL IFN- $\gamma$ , 50 ng/mL IFN- $\gamma$  + anti-IFN- $\gamma$ R1, or 50 ng/mL IFN- $\gamma$  + anti-IFN- $\gamma$ R1 + T cells for 48 hours. (K) THP-1 cells were treated with vehicle (PBS), 50 ng/mL IFN- $\gamma$ , 50 ng/mL IFN- $\gamma$  + anti-IFN- $\gamma$ R1, or 50 ng/mL IFN- $\gamma$  + anti-IFN- $\gamma$ R1 + T cells for 48 hours. (L) AML-250167 cells were treated with vehicle (PBS), 50 ng/mL IFN- $\gamma$ , 50 ng/mL IFN- $\gamma$  + anti-IFN- $\gamma$ R1, or 50 ng/mL IFN- $\gamma$  + anti-IFN- $\gamma$ R1 + T cells for 48 hours. (M) THP-1 cells were treated with vehicle (PBS), 50 ng/mL IFN- $\gamma$ , 50 ng/mL IFN- $\gamma$  + anti-IFN- $\gamma$ R1, or 50 ng/mL IFN- $\gamma$  + anti-IFN- $\gamma$ R1 + T cells for 48 hours. (N) THP-1 cells were treated with vehicle (PBS), 50 ng/mL IFN- $\gamma$ , 50 ng/mL IFN- $\gamma$  + anti-IFN- $\gamma$ R1, or 50 ng/mL IFN- $\gamma$  + anti-IFN- $\gamma$ R1 + T cells for 48 hours. (O) AML-250167 cells were treated with vehicle (PBS), 50 ng/mL IFN- $\gamma$ , 50 ng/mL IFN- $\gamma$  + anti-IFN- $\gamma$ R1, or 50 ng/mL IFN- $\gamma$  + anti-IFN- $\gamma$ R1 + T cells for 48 hours. (P) AML-250167 cells were treated with vehicle (PBS), 50 ng/mL IFN- $\gamma$ , 50 ng/mL IFN- $\gamma$  + anti-IFN- $\gamma$ R1, or 50 ng/mL IFN- $\gamma$  + anti-IFN- $\gamma$ R1 + T cells for 48 hours.

**Figure 2 (continued)** human HLA-mismatched CD3<sup>+</sup> T cells (E:T of 1:1), or FLZ and human T cells (FLZ + T) for 48 hours in the presence or absence of antibodies to human IFN- $\gamma$  (100  $\mu$ g/mL) and the IFN- $\gamma$ R1 or CD119 (10  $\mu$ g/mL). Isotype control antibodies were used as a negative control. MHC-II rMFI on the THP-1 (G) and AML-250167 (H) cells was measured by flow cytometry. (I-J) THP-1 IFN- $\gamma$ R1 (I) and  $\beta$ -actin (J) KO cell lines were generated using CRISPR-Cas9. Specifically, a lentivirus expressing CAS9, red-fluorescent protein (RFP), and IFN- $\gamma$ R1 or  $\beta$ -actin single guide RNA was used to infect THP-1 cells. IFN- $\gamma$ R1 KO (RFP<sup>+</sup>; IFN $\gamma$ R1<sup>-</sup>) and wild-type (RFP<sup>-</sup>; IFN- $\gamma$ R1<sup>+</sup>) cells or  $\beta$ -actin KO (RFP<sup>+</sup>;  $\beta$ -actin<sup>-</sup>) and wild-type (RFP<sup>-</sup>;  $\beta$ -actin<sup>+</sup>) cells were treated with vehicle (PBS), 50 ng/mL IFN- $\gamma$ , human HLA-mismatched CD3<sup>+</sup> T cells (E:T of 1:1), or FLZ and human T cells (FLZ + T) for 48 hours, and THP-1 MHC-II rMFI was determined by flow cytometry. (K-L) THP-1 (K) or AML-250167 (L) cells were treated with vehicle (PBS), 50 ng/mL IFN- $\gamma$ , human HLA-mismatched CD3<sup>+</sup> T cells (E:T of 1:1), or FLZ and human T cells (FLZ + T) for 48 hours in the presence or absence of ruxolitinib (1000 nM) or baricitinib (1000 nM). MHC-II rMFI on the THP-1 (K) and AML-250167 (L) cells was determined by flow cytometry. (M-P) THP-1 (M-N) or AML-250167 (O-P) cells were added to the upper and bottom chambers of a transwell plate with a 0.4- $\mu$ m pore size to prevent cell migration. Cells in the upper chamber were treated with vehicle (PBS), 50 ng/mL IFN- $\gamma$ , human HLA-mismatched CD3<sup>+</sup> T cells (E:T of 1:1), or FLZ and human T cells (FLZ + T) for 24 hours and MHC-II rMFI on an aliquot of the THP-1 (M) and AML-250167 (O) cells in both the upper and lower chambers was determined by flow cytometry. Remaining THP-1 (N) and AML-250167 (P) cells in the lower chamber were cultured for an additional 3 days in the absence of the upper chambers and MHC-II rMFI was determined longitudinally by flow cytometry. Bars represent means and error bars represent standard errors above and below (when applicable) the mean. *P* values were calculated using an unpaired, 2-sided Student *t* test. \**P* < .05; \*\**P* < .001; \*\*\**P* < .0001; \*\*\*\**P* < .00001.

decrease or variable expression (supplemental Figure 5). Transient and sustained increases in HLA-DR expression appear to correspond with serum IFN- $\gamma$  concentrations.

### T-cell immunotherapy-induced MHC-II expression is mediated by IFN- $\gamma$

FLZ + T or CART-123 treatment significantly increased IFN- $\gamma$  supernatant levels in vitro (Figure 2A-F). Addition of antibodies neutralizing IFN- $\gamma$  and IFN- $\gamma$ R1 (CD119) to the THP-1 and AML-250167 in vitro cocultures inhibited MHC-II upregulation (Figure 2G-H). Furthermore, KO of IFN- $\gamma$ R1, but not  $\beta$ -actin, in THP-1 cells inhibited FLZ + T and IFN- $\gamma$  from upregulating MHC-II (Figure 2I-J). Given that IFN- $\gamma$  signals through the JAK-STAT pathway, the JAK1/2 inhibitors ruxolitinib and baricitinib were added to the THP-1 and AML-250167 cocultures and also inhibited MHC-II upregulation (Figure 2K-L).<sup>21</sup>

We next hypothesized that soluble IFN- $\gamma$  produced by FLZ-activated T cells would upregulate MHC-II on bystander AML targets not directly contacted by T cells and FLZ. To test this hypothesis, we placed THP-1, FLZ, and T cells (or relevant controls) in the top well of a transwell plate and bystander THP-1 cells in the bottom well. THP-1 cells in both the top and bottom wells demonstrated MHC-II upregulation (Figure 2M). THP-1 cells in the bottom well were then replated, and MHC-II expression was measured serially in the absence of the cytotoxic effects of FLZ and T cells. MHC-II expression peaked at 48 to 72 hours (Figure 2N). Similar results were observed with AML-250167 (Figure 2O-P). Finally, we found that THP-1 cells treated with IFN- $\gamma$  to induce MHC-II upregulation stimulated HLA-mismatched CD4<sup>+</sup> T-cell proliferation to a greater degree than THP-1 cells that were not treated with IFN- $\gamma$  (supplemental Figure 6).

We demonstrated that FLZ and CAR-T cells targeting CD123, CD33, and CD371 upregulate MHC-II expression on AML blasts in vitro and in vivo. We identified IFN- $\gamma$  as the mediator of this effect, and blockade of IFN- $\gamma$  through the use of blocking antibodies, KO of IFN- $\gamma$ R1, or inhibition of IFN- $\gamma$  signaling via blockade of the JAK/STAT pathway prevented FLZ-mediated MHC-II upregulation. Bispecific antibodies represent a promising treatment option for the treatment of relapsed and refractory acute leukemias.<sup>16,22</sup> We provide a novel rationale for the use of IFN- $\gamma$ , bispecific T-cell engagers, bispecific antibodies, CAR-T, and other T-cell immunotherapies in the posttransplant relapse setting, not only to debulk the malignancy but also to reverse epigenetic MHC-II downregulation on AML blasts and reinvigorate graft-versus-malignancy effect. Encouragingly, we observed significant upregulation of MHC-II on AML blasts in primary human peripheral blood mononuclear cell samples

containing very few autologous T cells (E:T ratios as low as 1:61). Clinical trial testing of exogenous IFN- $\gamma$  (ClinicalTrials.gov ID NCT04628338) or FLZ (ClinicalTrials.gov ID NCT04582864) to treat AML or MDS relapse after allo-HCT are ongoing.

### Acknowledgments

The authors thank the Siteman Flow Cytometry Core for assistance with flow cytometry and the Division of Comparative Medicine at Washington University for their excellent animal care.

This work was supported by grants from the National Institutes of Health, National Cancer Institute (NCI): K08 Program grant (CA222630-01, to M.J.C.), NCI Research Specialist Award (R50 CA211466, to M.P.R.), a Genomics of Acute Myeloid Leukemia Program Project grant (P01 CA101937, to J.F.D.), and an NCI Outstanding Investigator Award (R35 CA197561, to J.F.D.).

### Authorship

Contribution: J.C.R., E.C., and M.P.R. designed and performed experiments, analyzed data, and wrote the manuscript; R.J. analyzed the single cell RNA-seq data and wrote the manuscript; M.J.C., J.K.R., S.C., and M.Y.K. designed and performed experiments; E.B. contributed flotetuzumab; and J.F.D. supervised the project, designed the research, and reviewed and edited the manuscript.

Conflict-of-interest disclosure: J.F.D. receives research funding from NeolimmuneTech, MacroGenics, Incyte, Bioline Rx; has equity ownership in Magenta Therapeutics, Wugen; and is a board member for hC Bioscience Inc, RiverVest Venture Partners. E.B. is an employee of MacroGenics, Inc, and receives compensation, stock, and stock options as condition of employment. The remaining authors declare no competing financial interests.

ORCID profile: R.J., 0000-0003-2368-4890.

Correspondence: John F. DiPersio, Division of Oncology, Washington University School of Medicine, 660 South Euclid Ave, Campus Box 8007, St. Louis, MO 63110; email: [jdipersi@wustl.edu](mailto:jdipersi@wustl.edu).

### Footnotes

Submitted 15 July 2022; accepted 15 November 2022; prepublished online in *Blood* First Edition 23 December 2022. <https://doi.org/10.1182/blood.2022017795>.

The authors are happy to share data from this manuscript with other investigators. If interested, investigators should send an email to the corresponding author.

The online version of this article contains a data supplement.

There is a [Blood Commentary](#) on this article in this issue.

The publication costs of this article were defrayed in part by page charge payment. Therefore, and solely to indicate this fact, this article is hereby marked "advertisement" in accordance with 18 USC section 1734.

## REFERENCES

1. Devillier R, Crocchiolo R, Etienne A, et al. Outcome of relapse after allogeneic stem cell transplant in patients with acute myeloid leukemia. *Leuk Lymphoma*. 2013;54(6):1228-1234.
2. Pollyea DA, Artz AS, Stock W, et al. Outcomes of patients with AML and MDS who relapse or progress after reduced intensity allogeneic hematopoietic cell transplantation. *Bone Marrow Transplant*. 2007;40(11):1027-1032.
3. Thanarajasingam G, Kim HT, Cutler C, et al. Outcome and prognostic factors for patients who relapse after allogeneic hematopoietic stem cell transplantation. *Biol Blood Marrow Transplant*. 2013;19(12):1713-1718.
4. Schmid C, de Wreede LC, van Biezen A, et al. Outcome after relapse of myelodysplastic syndrome and secondary acute myeloid leukemia following allogeneic stem cell transplantation: a retrospective registry analysis on 698 patients by the Chronic Malignancies Working Party of the European Society of Blood and Marrow Transplantation. *Haematologica*. 2018;103(2):237-245.
5. Christopher MJ, Petti AA, Rettig MP, et al. Immune escape of relapsed AML cells after allogeneic transplantation. *N Engl J Med*. 2018;379(24):2330-2341.
6. Toffalori C, Zito L, Gambacorta V, et al. Immune signature drives leukemia escape and relapse after hematopoietic cell transplantation. *Nat Med*. 2019;25(4):603-611.
7. Toffalori C, Cavattoni I, Deola S, et al. Genomic loss of patient-specific HLA in acute myeloid leukemia relapse after well-matched unrelated donor HSCT. *Blood*. 2012;119(20):4813-4815.
8. Matte-Martone C, Liu J, Zhou M, et al. Differential requirements for myeloid leukemia IFN- $\gamma$  conditioning determine graft-versus-leukemia resistance and sensitivity. *J Clin Invest*. 2017;127(7):2765-2776.
9. Chichili GR, Huang L, Li H, et al. A CD3 $\times$ CD123 bispecific DART for redirecting host T cells to myelogenous leukemia: preclinical activity and safety in nonhuman primates. *Sci Transl Med*. 2015;7(289):289ra82.
10. Al-Hussaini M, Rettig MP, Ritchey JK, et al. Targeting CD123 in acute myeloid leukemia using a T-cell-directed dual-affinity retargeting platform. *Blood*. 2016;127(1):122-131.
11. Choi J, Ritchey J, Prior JL, et al. In vivo administration of hypomethylating agents mitigate graft-versus-host disease without sacrificing graft-versus-leukemia. *Blood*. 2010;116(1):129-139.
12. Klco JM, Spencer DH, Lamprecht TL, et al. Genomic impact of transient low-dose decitabine treatment on primary AML cells. *Blood*. 2013;121(9):1633-1643.
13. Néron S, Thibault L, Dussault N, et al. Characterization of mononuclear cells remaining in the leukoreduction system chambers of apheresis instruments after routine platelet collection: a new source of viable human blood cells. *Transfusion*. 2007;47(6):1042-1049.
14. Kim MY, Jayasinghe R, Devenport JM, et al. A long-acting interleukin-7, rIL-7-hyFc, enhances CAR T cell expansion, persistence, and anti-tumor activity. *Nat Commun*. 2022;13(1):3296.
15. Heckl D, Kowalczyk MS, Yudovich D, et al. Generation of mouse models of myeloid malignancy with combinatorial genetic lesions using CRISPR-Cas9 genome editing. *Nat Biotechnol*. 2014;32(9):941-946.
16. Uy GL, Aldoss I, Foster MC, et al. Flotetuzumab as salvage immunotherapy for refractory acute myeloid leukemia. *Blood*. 2021;137(6):751-762.
17. Vadakekolathu J, Minden MD, Hood T, et al. Immune landscapes predict chemotherapy resistance and immunotherapy response in acute myeloid leukemia. *Sci Transl Med*. 2020;12(546):eaaz0463.
18. Vadakekolathu J, Lai C, Reeder S, et al. TP53 abnormalities correlate with immune infiltration and associate with response to flotetuzumab immunotherapy in AML. *Blood Adv*. 2020;4(20):5011-5024.
19. Klco JM, Spencer DH, Miller CA, et al. Functional heterogeneity of genetically defined subclones in acute myeloid leukemia. *Cancer Cell*. 2014;25(3):379-392.
20. Cui Zhou D, Jayasinghe RG, Chen S, et al. Spatially restricted drivers and transitional cell populations cooperate with the microenvironment in untreated and chemo-resistant pancreatic cancer. *Nat Genet*. 2022;54(9):1390-1405.
21. Choi J, Ziga ED, Ritchey J, et al. IFN $\gamma$ R signaling mediates alloreactive T-cell trafficking and GVHD. *Blood*. 2012;120(19):4093-4103.
22. Kantarjian H, Stein A, Gökbuget N, et al. Blinatumomab versus chemotherapy for advanced acute lymphoblastic leukemia. *N Engl J Med*. 2017;376(9):836-847.

© 2023 by The American Society of Hematology